likely to us that monopoles, with a charge n of less than 4 and a mass less than 15 BeV/c^2, probably do not exist.

Note added in proof. Since the monopole flux rates are well-defined measurements not subject to model-dependent interpretations, these rates should be used as a basis for comparison with other cosmic-ray experiments. The upper limit on the rate reported in the present experiment is smaller than that reported by Malkus[12] by a factor of 7000, and smaller than the rate estimated by Goto *et al.*[13] by a factor of about 20. In an accelerator experiment, Purcell *et al.*[9] set a cross limit about two orders of magnitude lower than our estimated cross section for 3 BeV/c^2 monopoles. The accelerator proton flux at 30 BeV was 80 times larger than our flux at 30 BeV and above.

ACKNOWLEDGMENTS

The authors gratefully acknowledge the helpful discussions they have enjoyed with Dr. J. Hornbostel, Dr. H. Kasha, Dr. L. Leipuner, and Dr. C. Hawkins. We would praticularly like to thank R. Larsen for his superior technical support.

PHYSICAL REVIEW VOLUME 149, NUMBER 4 30 SEPTEMBER 1966

Differential Cross Sections for $\pi^{\pm}p$ Elastic Scattering in the Momentum Range 875–1579 MeV/c

P. J. DUKE, D. P. JONES, M. A. R. KEMP, P. G. MURPHY,* J. D. PRENTICE,† AND J. J. THRESHER

Rutherford High Energy Laboratory, Chilton, Didcot, Berkshire, England

(Received 7 March 1966)

Measurements have been made of the differential cross sections for π^+p and π^-p elastic scattering at incident beam momenta in the range 875 to 1579 MeV/c. Two arrays of scintillation counters were used to detect pions scattered from a liquid-hydrogen target in coincidence with recoiling protons. In each of the 25 angular distributions, data were obtained at 18 center-of-mass angles varying from $\cos\theta^*=-0.97$ to $\cos\theta^*=0.75$. The differential cross sections have been expressed as series of the form $d\sigma^{\pm}/d\Omega=\sum_n C_n^{\pm}P_n \times(\cos\theta^*)$. The energy dependence of the coefficients $C_n^{\pm}$ suggests that $N^*(1688)$ has $J=\frac{5}{2}$, $I=\frac{1}{2}$, that $N^*(1928)$ has $J=\frac{7}{2}$, $I=\frac{3}{2}$, and that these two resonances have the same parity. The "shoulder" in the π^+p total cross section at about 950 MeV/c probably occurs in a $J=\frac{1}{2}$ wave.

I. INTRODUCTION

IN recent years extensive evidence has been obtained for the occurrence of resonant states in the πN system. Some of this evidence is plotted in Fig. 1 which shows the π^-p and π^+p total cross sections in the range 500–2500 MeV/c.[1–17] The figure also indicates the momenta at which differential cross sections and polarization measurements have been made. Obvious features in the π^-p channel are the peaks at 730

* Present address: Department of Physics, The University, Manchester 13, England.

† Present address: Department of Physics, University of Toronto, Toronto 5, Canada.

[1] F. Bulos, R. E. Lanou, A. E. Pifer, A. M. Shapiro, M. Widgoff, R. Panvini, A. E. Brenner, C. A. Bordner, M. E. Law, E. E. Ronat, K. Strauch, J. Szymanski, P. Bastien, B. B. Brabson, Y. Eisenberg, B. T. Feld, V. K. Fischer, I. A. Pless, L. Rosenson, R. K. Yamamoto, G. Calvelli, L. Guerriero, G. A. Salandin, A. Tomasin, L. Ventura, C. Voci, and F. Waldner, Phys. Rev. Letters **13**, 558 (1964).

[2] R. W. Kenney, C. B. Chiu, R. D. Eandi, B. J. Moyer, J. A. Poirier, W. B. Richards, R. J. Cence, V. Z. Peterson, and V. J. Stenger, Bull. Am. Phys. Soc. **9**, 409 (1964).

[3] D. E. Damouth, L. W. Jones, and M. L. Perl, Phys. Rev. Letters **11**, 287 (1963).

[4] R. D. Eandi, T. J. Devlin, R. W. Kenney, P. G. McManigal, and B. J. Moyer, Lawrence Radiation Laboratory Report No. UCRL-11501 (unpublished).

[5] R. D. Eandi, T. J. Devlin, R. W. Kenney, P. G. McManigal, and B. J. Moyer, Phys. Rev. **136**, B536 (1964).

[6] J. A. Helland, T. J. Devlin, D. E. Hagge, M. J. Longo, B. J. Moyer, and C. D. Wood, Phys. Rev. **134**, B1062 (1964).

[7] J. A. Helland, C. D. Wood, T. J. Devlin, D. E. Hagge, M. J. Longo, B. J. Moyer, and V. Perez-Mendez, Phys. Rev. **134**, B1079 (1964).

[8] P. M. Ogden, Lawrence Radiation Laboratory Report No. UCRL-11180 (unpublished).

[9] E. H. Bellamy, T. F. Buckley, W. Busza, D. G. Davies, B. G. Duff, F. F. Heymann, P. V. March, C. C. Nimmon, A. Stefanini, J. A. Strong, R. N. F. Walker, and D. T. Walton, Proc. Roy. Soc. (London) **A289**, 509 (1966).

[10] A. S. Carroll, A. B. Clegg, I. F. Corbett, C. J. S. Damerell, N. Middlemas, D. Newton, T. W. Quirk, and W. S. C. Williams, Proc. Roy. Soc. (London) **A289**, 513 (1966).

[11] P. Bareyre, Proc. Roy. Soc. (London) **A289**, 463 (1966).

[12] P. Bareyre, C. Bricman, M. J. Longo, G. Valladas, G. Villet, G. Bizard, J. Duchon, J. M. Fontaine, J. P. Patry, J. Seguinot, and J. Yonnet, Phys. Rev. Letters **14**, 878 (1965).

[13] T. J. Devlin, J. Solomon, and G. Bertsch, Phys. Rev. Letters **14**, 1031 (1965).

[14] J. C. Brisson, J. F. Detoeuf, P. Falk-Vairant, L. van Rossum, G. Valladas, and L. C. L. Yuan, Phys. Rev. Letters **3**, 561 (1959).

[15] T. J. Devlin, B. J. Moyer, and V. Perez-Mendez, Phys. Rev. **125**, 690 (1962).

[16] A. N. Diddens, E. W. Jenkins, T. F. Kycia, and K. F. Riley, Phys. Rev. Letters **10**, 262 (1963).

[17] A. Stirling *et al.* (to be published). For a tabulation of the data see B. Amblard, P. Borgeaud, Y. Ducros, P. Falk-Vairant, O. Guisan, W. Laskar, P. Sonderegger, A. Stirling, M. Yvert, A. Tran Ha, and S. D. Warshaw, Phys. Letters **10**, 138 (1964).

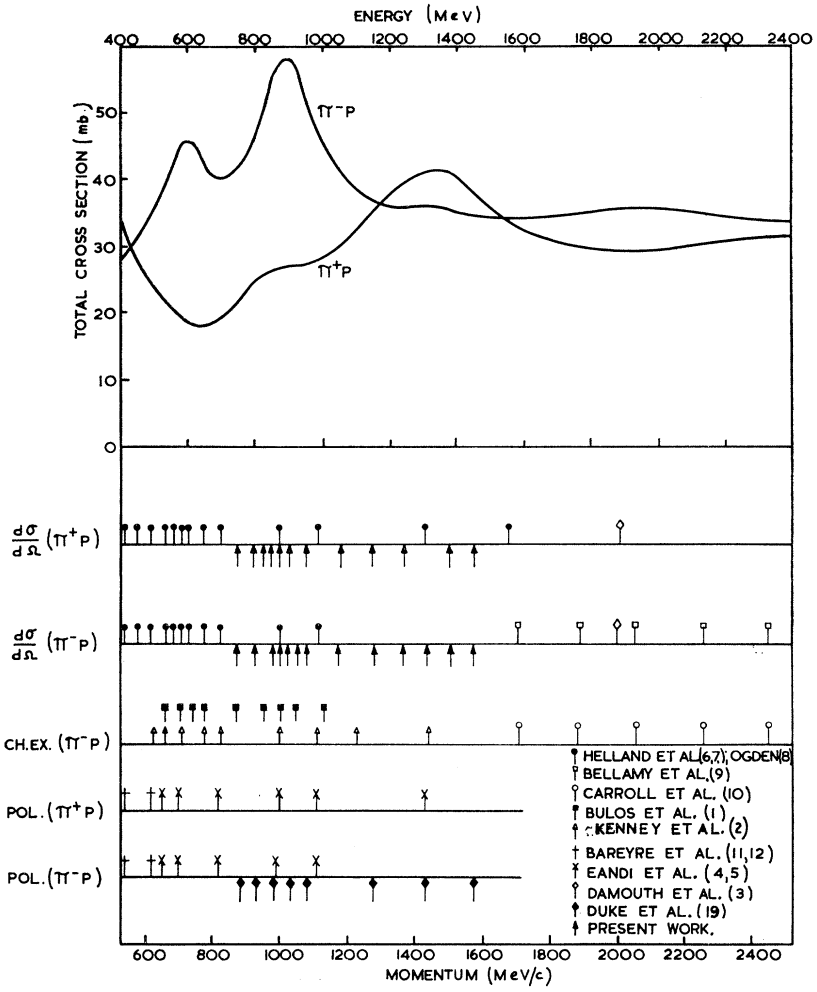

FIG. 1. Total $\pi^- p$ and $\pi^+ p$ cross sections showing energies at which differential cross section and polarization measurements have been made. For details of the total cross section measurements see Refs. 12–17.

MeV/c and 1030 MeV/c, conventionally attributed to to the formation of the resonant states $N^*(1514)$ and $N^*(1688)$. In the $\pi^+ p$ channel, there is a peak at about 1480 MeV/c [$N^*(1928)$] and a shoulder at 950 MeV/c.

It has not previously been possible to make parity assignments to the $N^*(1688)$ and $N^*(1928)$ states. In order to obtain these quantum numbers a series of measurements has been made at Nimrod of differential cross sections and polarization effects for $\pi^\pm p$ elastic scattering in the momentum range 875–1579 MeV/c. Preliminary reports have already been given[18,19]; the present paper reports in detail the results of the differential cross section measurements.

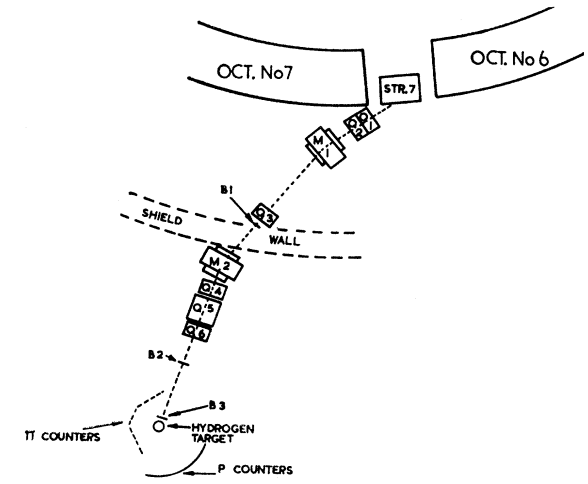

FIG. 2. Beam layout (not to scale).

II. EXPERIMENTAL ARRANGEMENT

Figure 2 shows the layout of the beam. Pions were produced by causing the Nimrod internal beam to strike a beryllium target placed in one of the straight sections. This target was 10 cm long×1.5 cm wide×0.6

[18] H. H. Atkinson, C. R. Cox, P. J. Duke, K. S. Heard, D. P. Jones, M. A. R. Kemp, P. G. Murphy, J. D. Prentice, and J. J. Thresher, Proc. Roy. Soc. (London) **A289**, 449 (1966).

[19] P. J. Duke, D. P. Jones, M. A. R. Kemp, P. G. Murphy, J. D. Prentice, J. J. Thresher, H. H. Atkinson, C. R. Cox, and K. S. Heard, Phys. Rev. Letters **15**, 468 (1965).

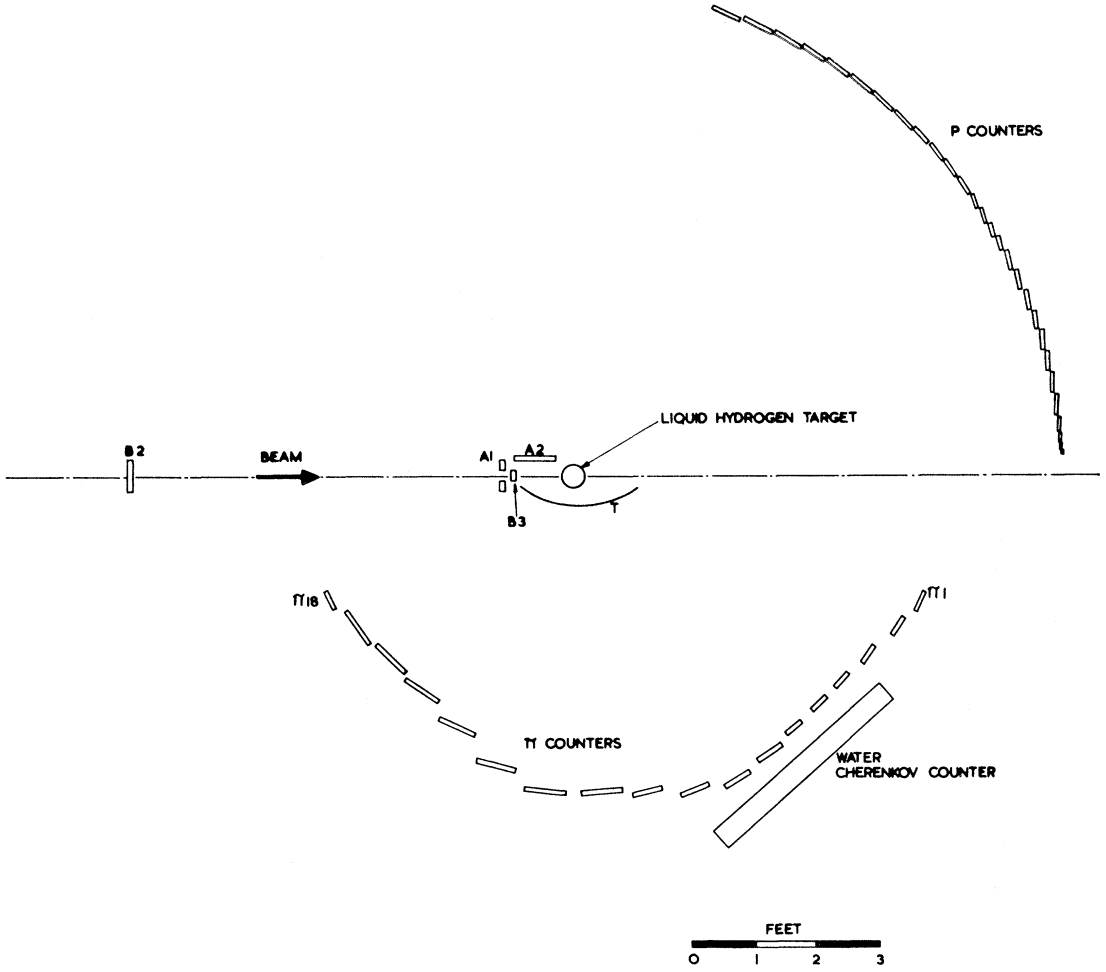

FIG. 3. Counter arrangement.

cm high; the pion production angle of 26° therefore gave an effective source 5 cm wide×0.6 cm high. The beam momentum was defined by counters $B1$, $B3$, and the bending magnet $M2$, calibrated to $\pm\frac{1}{2}\%$ by means of floating-wire measurements. A momentum dispersion at $B1$ of $2\frac{1}{2}\%$/inch was provided by the magnet $M1$. At 7.3 GeV internal beam energy, 10^{11} protons per Nimrod pulse incident on the beryllium target produced 30 000 π^- mesons per pulse at a mean momentum of 1030 MeV/c, with a momentum spread of $4\frac{1}{2}\%$ (full width at half-maximum).

The counter arrangement used is shown in Fig. 3. $B2$ and $B3$ defined the beam; $A1$ and $A2$ were veto counters which rejected events in which particles were scattered from points outside the fiducial volume of liquid hydrogen, which was defined in the vertical plane by $B3$. The scintillator in $B3$ was $\frac{1}{16}$ in. thick and was mounted in an air light-pipe. The inner vessel of the target was a vertical cylinder 4 in. high×4 in. in diameter, with walls of 0.01-in. Melinex and the outer vessel has a 0.05-in. Melinex window.

A trigger generated by the coincidence $B1$ $B2$ $B3$ T $\bar{A}1$ $\bar{A}2$ (with a resolving time of 7 nsec full width at half-maximum) indicated that a pion interacted in the liquid hydrogen to produce at least one charged particle moving through the counter T towards the π array. (Protons present in the beam for π^+ runs were rejected by the $B1$ $B2$ $B3$ timing requirement.) The event was recorded if in addition a count in one and only one π counter and a count in one and only one p counter were in coincidence with this trigger within an over-all resolving time of 20 nsec. The water Čerenkov counter, $WC(\pi)$, was used in coincidence with π counters in the laboratory angular range 36° to 65° to reject events in which protons scattered into these counters (see below). Figure 4 shows a block diagram of the electronics.

Solid angles for elastic scattering were defined by the π counters. The p counters were made slightly larger than necessary to count all the protons conjugate to elastically scattered pions. For each event, the outputs from the appropriate π counter and p counter were encoded to form a work of 9 binary bits. This word defined

an address in the core store of a Laben pulse-height analyzer and the contents of this address were then increased by one. In this way all possible coincidences between each π counter and any p counter were recorded. The deadtime associated with the recording of an event was 40 μsec. The accumulated information in the core store was typed out and also punched on paper tape at regular intervals. Typically, in one hour of running 4×10^6 incident pions produced $\approx10\,000$ stored events. Beam bursts were about 250 msec long with negligible rf structure. The repetition rate was 23 bursts per minute.

Typical plots of the coincidence rates in some of the π counters as a function of p counter number are shown in Fig. 5. For π counters with laboratory angles $\theta<90°$ it was possible to detect "reverse elastic" events in which the roles of the π and p arrays were interchanged. Just forward of 90° the kinematics (Fig. 6) were such that the forward and reverse elastic peaks were separated [Fig. 5(b)]. In the range $\theta=36°$ to $\theta=65°$, the water Čerenkov counter was used to reject protons which would otherwise have produced reverse elastic events overlapping the forward peak [Fig. 5(c)]. For $\theta<36°$ reverse elastic events either were separated, or did not appear because the pion was scattered through more than 90° and was not detected by the p array [Fig. 5(a)]. In the region $\theta>90°$ reverse elastic events were not possible [Fig. 5(d)].

III. CORRECTIONS TO THE DATA

Significant corrections to the basic data were needed to account for the following effects:

(A) Beam contamination
(B) Beam absorption
(C) Absorption of scattered particles
(D) T-counter efficiency
(E) Water counter efficiency
(F) Proton-counter geometry
(G) Detection of pions in π counter light-pipes
(H) Ionization loss of low-energy recoil protons
(I) Effective thickness of target.

A. Beam Contamination

For π^+ runs, 80% of the beam particles were protons. On account of the difference in times of flight between the protons and pions the protons failed to satisfy the $B1$ $B2$ $B3$ timing requirement. The contribution to the observed beam rate from accidental coincidences was measured to be $(3.5\pm1.0)\%$. There was also a 4% probability that a proton was at the target close enough in time to a pion (within 20 nsec) to simulate a genuine event if it scattered. This made it necessary to correct the observed rate in those forward π counters not in coincidence with $WC(\pi)$. Because of the differing kinematics of πp and pp scattering, at low momenta the pp peak for $\pi3$ was resolved from the πp peak. The

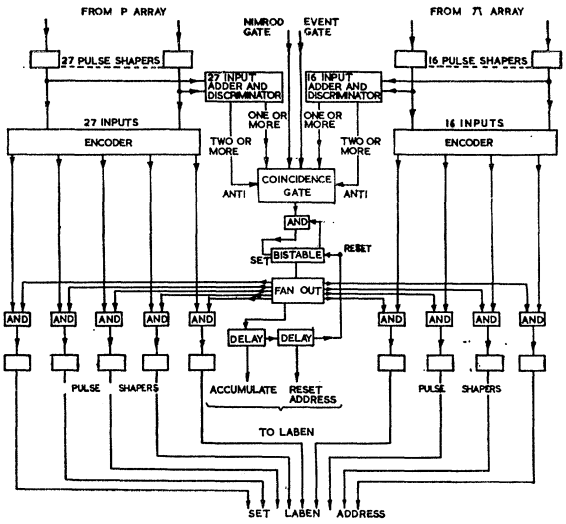

FIG. 4. Block diagram of electronics. In any one run only 16 of the 18 counters were connected.

height of the resolved pp peak was used to estimate the corrections for other counters and momenta using the known behavior of the pp differential cross sections.[20] In general the corrections were in the range 5–10%. The errors on the corrected points were increased by a factor 1.1 to allow for uncertainties in these calculations.

In addition both the π^+ and the π^- beams were contaminated with muons and electrons. The beam composition was analyzed with a gas Čerenkov counter filled with Arcton 13 ($CClF_3$) placed immediately upstream of $B3$. Information from curves of counting rate against gas pressure was supplemented by absorption measurements using iron plates. The total lepton contamination was found to vary between $(8\pm2)\%$ at 875 MeV/c and $(4\pm1)\%$ at 1579 MeV/c.

B. Beam Absorption

The pion flux reaching the center of the liquid-hydrogen target was less than that recorded owing to absorption in $B3$, the target walls, and the liquid hydrogen. The size of this effect, which depended on beam momentum and the sign of the charge of the incident pions, was about 1%.

C. Absorption of Scattered Particles

Absorption of the scattered pions in the target and counter T and of the recoil protons in the target was calculated from the known values of elastic and total cross sections. The effect was usually $\approx2\%$ except for low momentum π^+ runs where pions with large scattering angles had laboratory momenta close enough to the peak of the $\frac{3}{2}$-$\frac{3}{2}$ resonance (310 MeV/c) for the correction to be as large as 7%. In each case the uncertainty

[20] W. N. Hess, Rev. Mod. Phys. **30**, 368 (1958).

in the correction was negligible compared with the statistical accuracy of the data.

D. T-Counter Efficiency

This was measured to be $(99.0\pm0.5)\%$ for all pion scattering angles.

E. Water-Counter Efficiency

The water-counter was placed in a low-intensity π^- beam with the counters $\pi4$-$\pi8$ in the same positions relative to it as in normal operation. It was thus possible to measure in turn the efficiency of each of the five π-counter, water-counter combinations. The measurements gave results in the range 95 to 98% with uncertainties of $\pm\frac{1}{2}\%$.

F. Proton Counter Geometry

Ideally, the p array should have presented a continuous expanse of scintillator to recoil protons. On account of the "one and only one" requirement of the logic, overlaps due to misalignments and nonzero thicknesses of the scintillators were operationally indistinguishable from gaps between the counters. The corrections for losses due to these two effects were deduced from a survey of the counter positions, and were found to be in the range 0–5% (usually about 2%), with negligible uncertainty.

G. Detection of Pions in π Counter Light-Pipes

The heights of the p counters were slightly larger than required for two-body kinematics, to allow for multiple scattering of the particles. As a result, it was possible to count elastic events in which the pions were detected by means of Čerenkov light produced in the Perspex light-pipes of the π counters. For each π counter the counting efficiency was measured at various positions on the light-pipe over a range of incident beam momenta. The results were combined with geometrical factors to give over-all corrections which were usually about 1%. In two cases low-discrimination levels gave corrections of $(8\pm2)\%$.

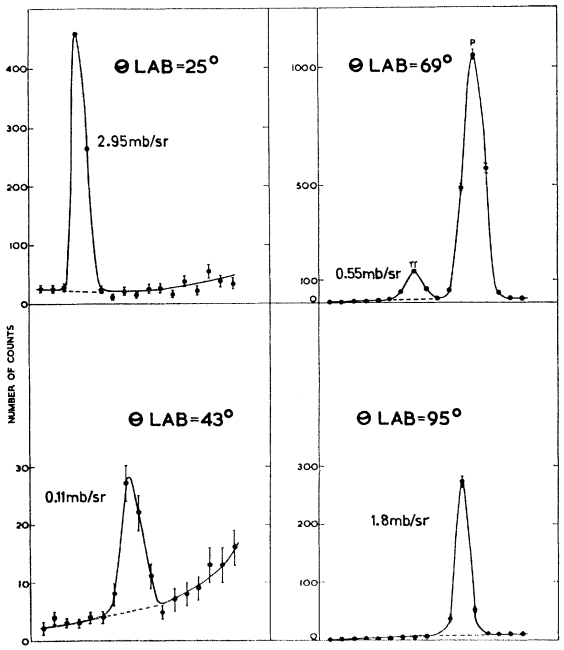

FIG. 5. Plots of typical coincidence counting rates between π and p counters. (a) $\theta=25°$; (b) $\theta=69°$; (c) $\theta=43°$; (d) $\theta=95°$.

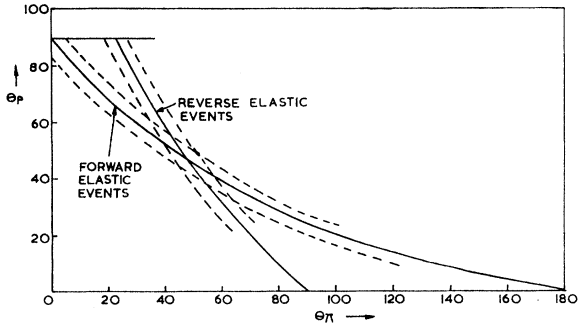

FIG. 6. Variation of proton scattering angle (θ_p) with pion scattering angle (θ_π) for a beam momentum of 1030 MeV/c showing forward and reverse kinematics. The dashed lines show approximately the effect of angluar resolution.

H. Ionization Loss of Low-Energy Recoil Protons

For beam momenta below 1080 MeV/c and elastically scattered pions reaching the most forward π counter, not all the recoil protons had sufficient energy to produce a count on reaching the scintillator of a p counter. Calculations of the required corrections were made and the estimated errors of the points affected were increased to allow for the uncertainty in the knowledge of this threshold energy and of the energy loss of the very low energy protons in the counter wrappings. In the worst case ($\cos\theta^*=0.823$ at 875 MeV/c) the correction factor was 1.25 ± 0.06; for $\cos\theta^*=0.811$ at 975 MeV/c it was 1.06 ± 0.04.

I. Effective Thickness of Target

The effective thickness of the target differed from the nominal diameter because of

(a) contraction on cooling to liquid-hydrogen temperatures, which amounted to a 0.6% effect,

(b) the horizontal extent of the beam. This gave a $(6.0\pm0.5)\%$ reduction, which came mainly from the curvature of the target walls. The correction was not very sensitive to the shape of the intensity distribution across the beam.

IV. CALCULATION OF DIFFERENTIAL CROSS SECTIONS

A computer program was written which calculated the center-of-mass differential cross sections from the

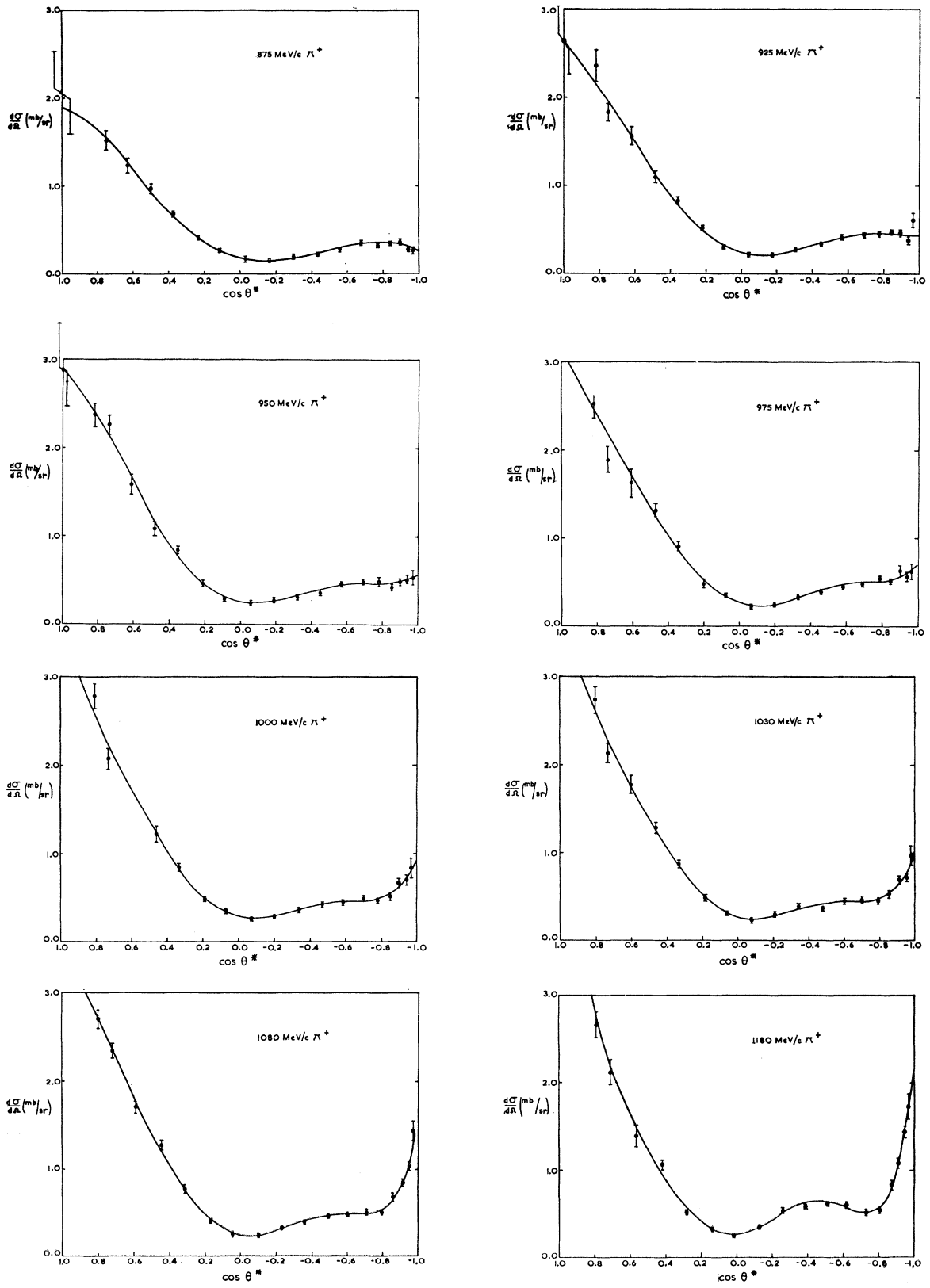

FIG. 7. Differential cross sections for $\pi^+ p$ elastic scattering.

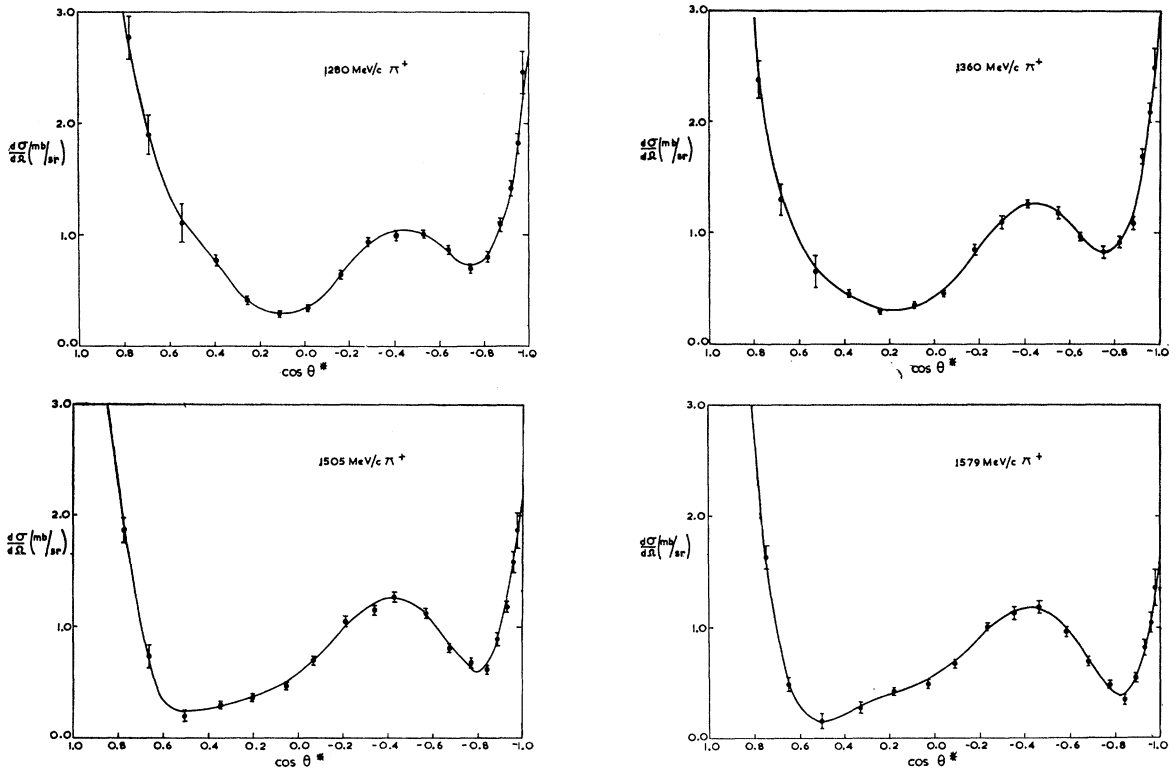

FIG. 7 (*continued*)

numbers of elastic events associated with the π-counters. Corrections were made for the effects discussed in Sec. 3 and for the presence of backgrounds. The latter were obtained for each momentum by fitting a surface to the experimental data in the space of counting rate versus π and p counter angles, the points inside the forward and reverse elastic peaks not being included. This surface was divided into three regions to allow for the discontinuities in the background caused by the water Cherenkov counter. It was then used to estimate the background under the elastic peaks and the appropriate subtractions were made.

V. RESULTS

The differential cross sections obtained are shown in Figs. 7 and 8. The points at 0° are taken from dispersion-relation calculations.[21]

VI. ANALYSIS OF THE DATA

The measured differential cross sections $d\sigma/d\Omega$ were expanded in terms of the Legendre polynomials $P_n(\cos\theta^*)$:

$$(d\sigma/d\Omega)(\pi^{\pm}p)=\sum_{n=0}^{n\max} C_n^{\pm}P_n(\cos\theta^*), \qquad (1)$$

where θ^* is the center-of-mass scattering angle. Values of the coefficients $C_n^{\pm}$ were obtained from a least-squares fitting program. Fits were made both with and without the forward point ($\theta^*=0°$) included. No statistically significant difference between the two sets of coefficients was found; the additional information present in the fits with the forward point included allowed considerably more precise values of the higher coefficients to be calculated.

The expansions were made in terms of the functions $P_n(\cos\theta^*)$ rather than $\cos^n\theta^*$ on account of the smaller correlations among the expansion coefficients obtained. The fitting program calculated values of the coefficients which minimized the quantity

$$\chi^2=\sum_i (1/\Delta r_i^2)[r_i-\sum_{n=0}^{n\max} C_n^{\pm}P_n(\cos\theta_i^*)]^2,$$

where $r_i\pm\Delta r_i$ is the measured cross section observed at angle θ_i^*. It is easily shown[22] that this is equivalent to solving for $C_n^{\pm}$ the equations

$$U_m=\sum_n C_n^{\pm}V_{nm},$$

where

$$U_m=\sum_i (r_i/\Delta r_i^2)P_m(\cos\theta_i^*)$$

and

$$V_{nm}=V_{mn}=\sum_i \Delta r_i^{-2}P_n(\cos\theta_i^*)P_m(\cos\theta_i^*). \qquad (2)$$

[21] C. Lovelace (private communication).

[22] J. Orear, University of California Radiation Laboratory Report No. UCRL 8417 (unpublished).

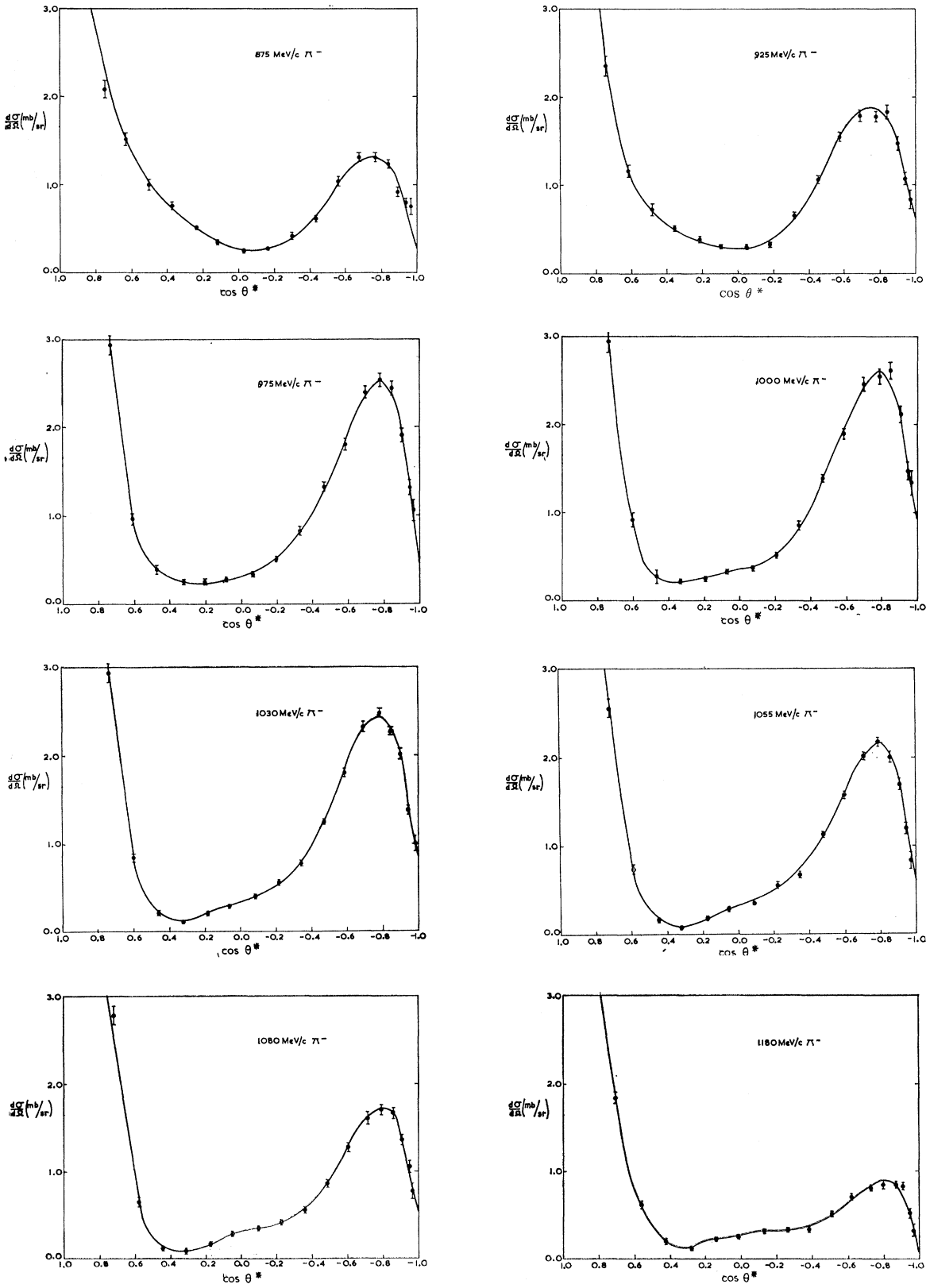

FIG. 8. Differential cross sections for $\pi^- p$ elastic scattering.

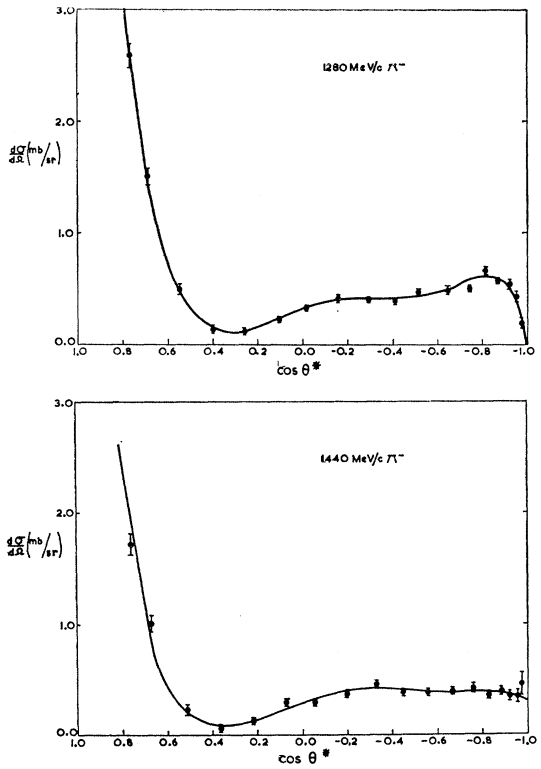

FIG. 8 (*continued*)

The error matrix E is defined by V^{-1}, in terms of which the rms errors ΔC_n are given by the diagonal elements

$$(\Delta C_n)^2 = E_{nn}. \tag{3}$$

The corrections between the coefficients are given by the off-diagonal elements. Thus the condition that for a given order of fit no correlation exists is that V_{nm} be diagonal. If

(a) the errors Δr_i are equal,

(b) the measurements are made over a large number of equally spaced values of $\cos\theta_i^*$ covering the whole range $-1 \leq \cos\theta_i^* \leq +1$

$$V_{nm} \rightarrow \frac{1}{\Delta r^2}\int_{-1}^{+1} P_n(\cos\theta^*)P_m(\cos\theta^*)d(\cos\theta^*) = \frac{1}{\Delta r^2}\frac{2\delta_{nm}}{2n+1}. \tag{4}$$

If expansions are made to order k and $k+1$, the values of the coefficient $C_n^{\pm}(n \leq k)$ obtained in the two cases are given by

$$C_n^{\pm} = \sum_{m=0}^{k} (V^{-1})_{nm}U_m = (V^{-1})_{nn}U_n \text{ (no summation)}$$

and

$$C'^{\pm}_n = \sum_{m=0}^{k+1} (V'^{-1})_{nm}U_m = (V'^{-1})_{nm}U_n,$$

where V and V' are diagonal matrices of order $k+1$ and $k+2$, respectively. From Eq. (4) it follows that $(V^{-1})_{nn} = (V'^{-1})_{nn}$ for $n \leq k$. Therefore,

$$C_n^{\pm} = C_n'^{\pm} \quad \text{for} \quad n \leq k.$$

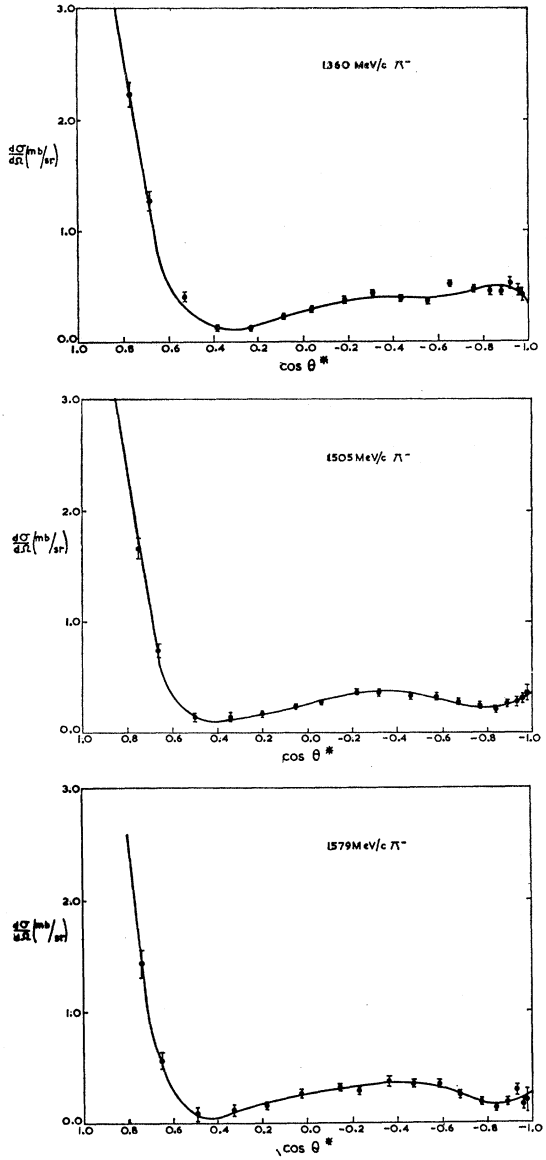

FIG. 8 (*continued*)

In practice the independence of the coefficients is remarkably high, even though the matrix V has appreciable off-diagonal elements. The value of $n_{\max}$ required at a given momentum was deduced from the behavior of the goodness-of-fit parameter $G = \chi^2/d$, where

d = No. of degrees of freedom
= (No. of points fitted $-n_{\max}-1$).

χ^2 has a Gaussian distribution with mean d and standard deviation $(2d)^{1/2}$. Thus G should have mean 1 and stand-

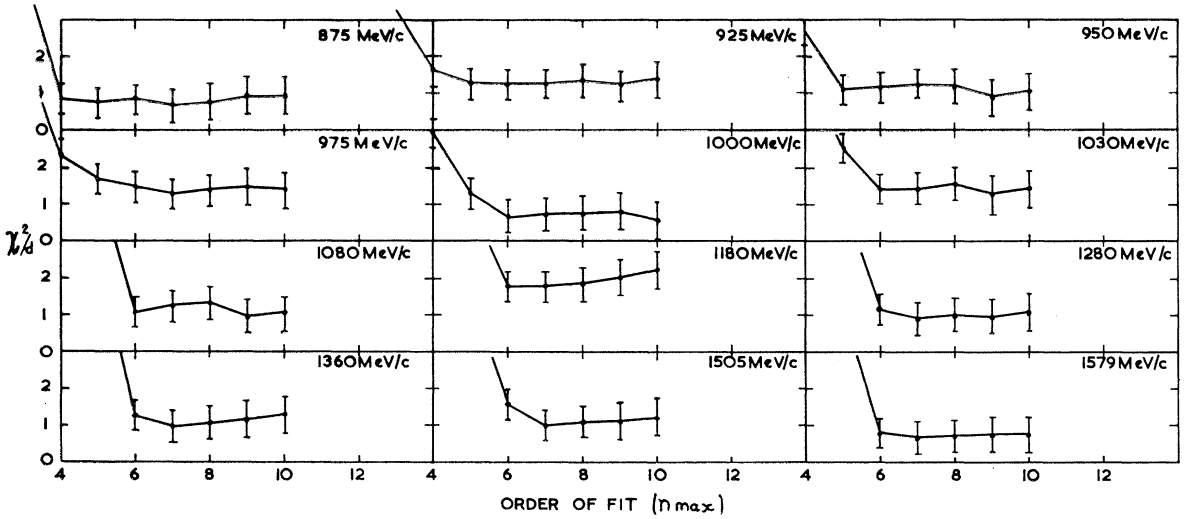

FIG. 9. Goodness-of-fit parameter G for π^+p elastic scattering.

ard deviation $(2/d)^{1/2}$ for correctly chosen $n_{\max}$ and well estimated errors Δr_i. The choice of $n_{\max}$ for each momentum was made by inspection, bearing in mind the expected fluctuations in G. Figures 9 and 10 show the variation of G with $n_{\max}$ for each of the 25 angular distributions, and Table I contains the values of $n_{\max}$ finally chosen. The distribution of $(G-1)$ appropriate to these values of $n_{\max}$ is shown in Fig. 11, and angular distributions calculated from the corresponding values of $C_n^{\pm}$ are plotted as continuous curves in Figs. 7 and 8. Distributions of the deviations of the experimental points from the fitted curves are shown in Fig. 12. These are consistent with the expected Gaussian distributions. Two of the 450 points were about three standard deviations from the fitted curves. [These two points ($\cos\theta^*=0.823$ for 875-MeV/c π^+ and $\cos\theta^*=0.602$ for 1000-MeV/c π^+) were rejected and the final fits obtained without them.]

Figures 13 and 14 give the behavior of $C_n^{\pm}$ as functions of momentum. Discontinuities in the higher order coefficients have been avoided by plotting the results obtained from 7th-order fits throughout, even though 5th- or 6th-order fits were adequate in many cases. This procedure did not cause significant changes in the values of the coefficients obtained from the lower order fits.

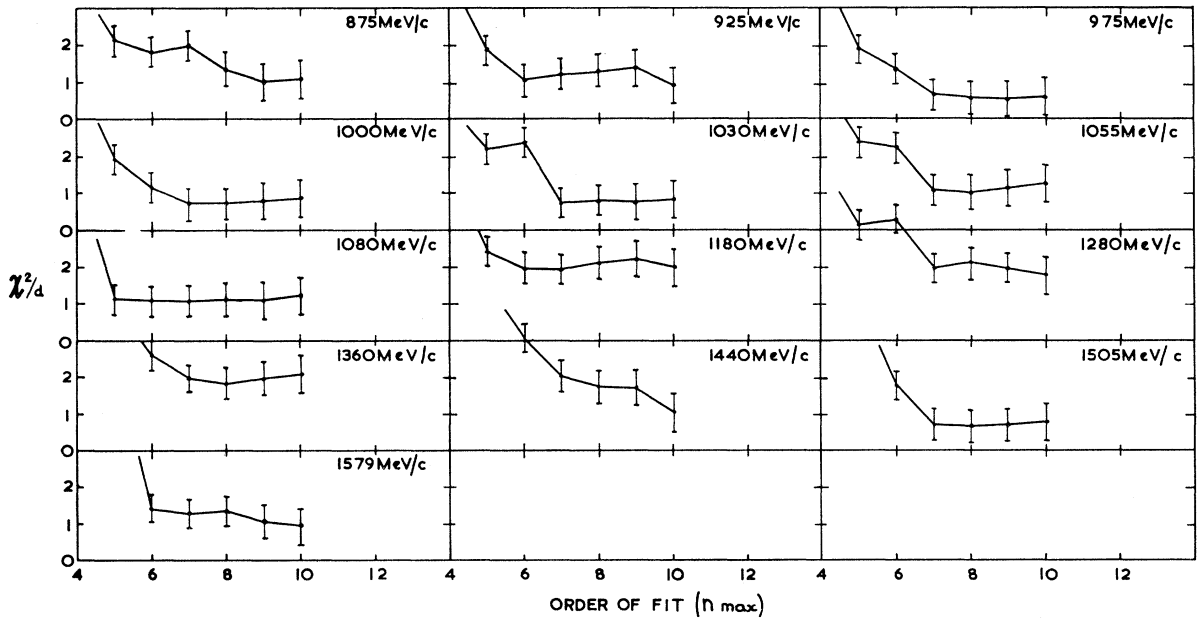

FIG. 10. Goodness-of-fit parameter G for π^-p elastic scattering.

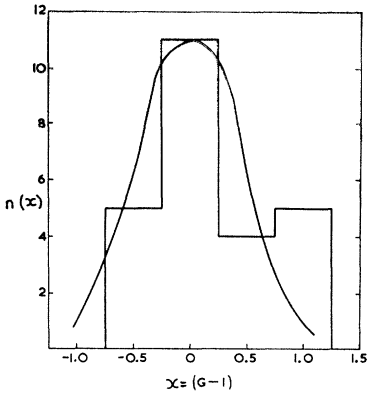

FIG. 11. Distribution of $x=(G-1)$ for the orders of fit shown in Table I. G is the goodness-of-fit parameter.

VII. INTERPRETATION OF RESULTS; SPINS OF $N^*(1688)$ AND $N^*(1928)$

A. General

The differential cross section may be written in the form

$$d\sigma/d\Omega = |f(\theta^*)|^2 + |g(\theta^*)|^2,$$

TABLE I. Orders of fit used to obtain the coefficients $C_n^{\pm}$ in the expressions $d\sigma^{\pm}/d\Omega = \sum_n C_n^{\pm} P_n(\cos\theta^*)$.

Momentum (MeV/c)	Order of fit π^-	π^+
875	5	5
925	6	5
950	...	5
975	7	6
1000	7	6
1030	7	6
1055	7	...
1080	7	6
1180	7	6
1280	7	6
1360	7	6
1440	7	...
1505	7	7
1579	7	7

TABLE II. Values of the coefficients $\alpha_n^{i,j}$ in the expansion. $d\sigma/d\Omega = \sum_n C_n P_n(\cos\theta^*) = \sum_{i\leq j,j} \alpha_n^{i,j} \mathrm{Re}(A_i^* A_j) P_n(\cos\theta^*)$.

A_iA_j	C_0	C_1	C_2	C_3	C_4	C_5	C_6	C_7	C_8
$S\,S$	1								
$P1\,S$		2							
$P1\,P1$	1								
$P3\,S$		4							
$P3\,P1$			4						
$P3\,P3$	2		2						
$D3\,S$			4						
$D3\,P1$		4							
$D3\,P3$		0.80		7.20					
$D3\,D3$	2		2						
$D5\,S$			6						
$D5\,P1$				6					
$D5\,P3$		7.20		4.80					
$D5\,D3$			1.71		10.29				
$D5\,D5$	3		3.43		2.57				
$F5\,S$				6					
$F5\,P1$			6						
$F5\,P3$			1.71		10.29				
$F5\,D3$		7.20		4.80					
$F5\,D5$		0.51		3.20		14.29			
$F5\,F5$	3		3.43		2.57				
$F7\,S$				8					
$F7\,P1$					8				
$F7\,P3$			10.29		5.71				
$F7\,D3$				2.67		13.33			
$F7\,D5$		10.29		8		5.71			
$F7\,F5$			1.14		4.68		18.18		
$F7\,F7$	4		4.76		4.21		3.03		
$G7\,S$					8				
$G7\,P1$				8					
$G7P3$				2.67		13.33			
$G7\,D3$			10.29		5.71				
$G7\,D5$			1.14		4.68		18.18		
$G7\,F5$		10.29		8		5.71			
$G7\,F7$		0.38		2.18		6.59		22.84	
$G7\,G7$	4		4.76		4.21		3.03		
$G9\,S$					10				
$G9\,P1$						10			
$G9\,P3$				13.33		6.67			
$G9\,D3$					3.64		16.36		
$G9\,D5$			14.29		9.35		6.36		
$G9\,F5$				1.82		6.15		22.03	
$G9\,F7$		13.33		10.91		9.23		6.53	
$G9\,G7$			0.87		3.24		8.48		27.41
$G9\,G9$	5		6.06		5.66		4.85		3.43

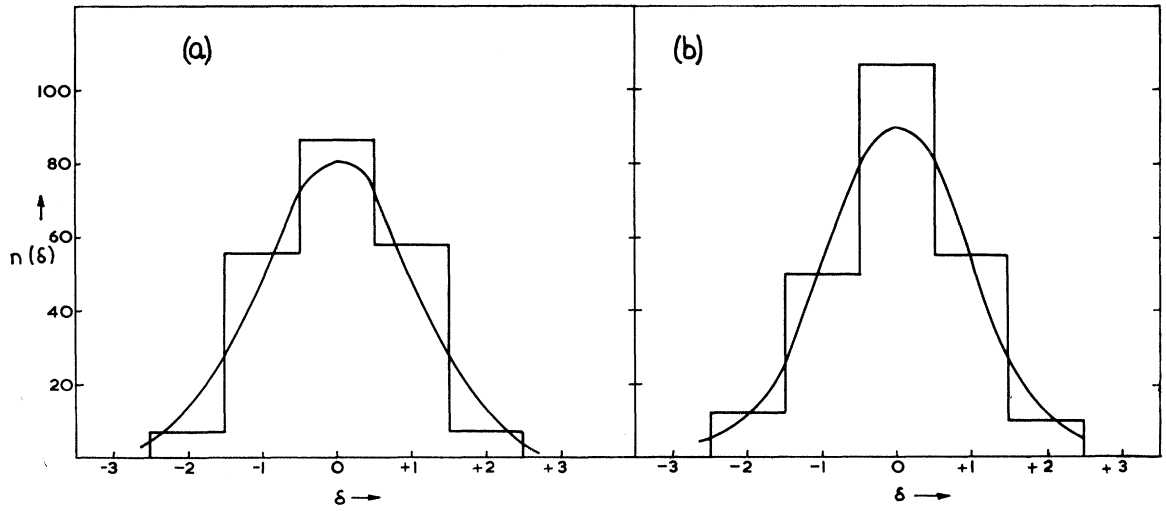

FIG. 12. Distributions of the deviations of the measured cross sections from the fitted curves for the orders of fit shown in Table I. (a) $\pi^+ p$; (b) $\pi^- p$.

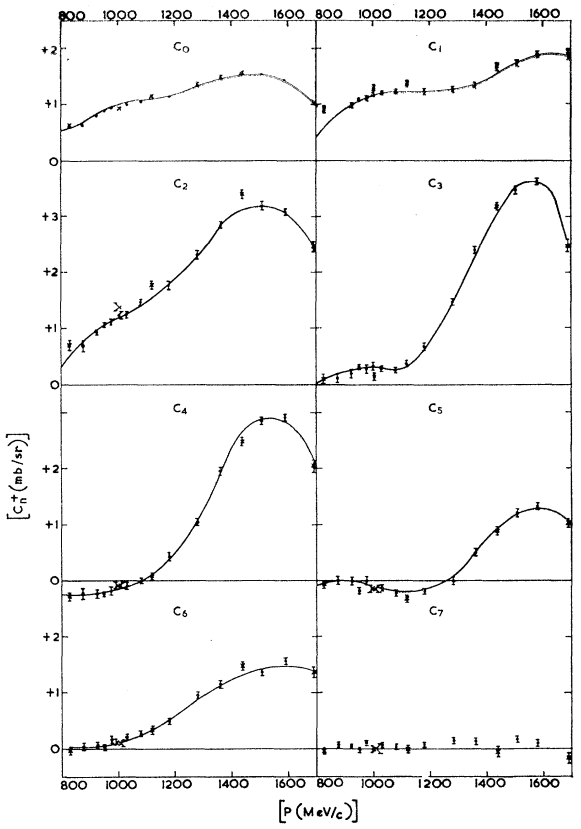

FIG. 13. Expansion coefficients for π^+p elastic scattering obtained from 7th-order fits at all momenta. The points denoted by crosses at 827, 1003, 1121, 1440, and 1690 MeV/c are taken from Helland *et al.* (Ref. 6).

where

$$f(\theta^*)=\sum_{l=0}^{L}[(l+1)A_{l+}+lA_{l-}]P_l(\cos\theta^*)$$

and

$$g(\theta^*)=\sum_{l=1}^{L}[A_{l+}-A_{l-}]\sin\theta^*P_l'(\cos\theta^*).$$

A_{l+} and A_{l-} are the scattering amplitudes for waves having $J=l+\frac{1}{2}$ and $J=l-\frac{1}{2}$ respectively. If $d\sigma/d\Omega$ is written in the form of Eq. (1), then $C_n^{\pm}=\sum_{i\leq j,j}\alpha_n{}^{i,j}\times\mathrm{Re}(A_i{}^*A_j)$. Here $A_i=A_{l+}$ etc. Table II gives the values of α for $l\leq 4$.

B. Spin of $N^*(1928)$; the "Shoulder" in π^+p Scattering

The main features of the coefficients plotted in Fig. 13 are the peaks at about 1480 MeV/c in $C_0{}^+$ to $C_6{}^+$; $C_7{}^+$ and $C_8{}^+$ (not shown) are very small. Detailed considerations of this behavior show that the only reasonable explanation is that the peaks are caused by a resonance in a $J=\frac{7}{2}$ partial wave amplitude.[19] The small values of the higher coefficients indicate that the nonresonant $J=\frac{7}{2}$ amplitude of opposite parity and all other amplitudes with larger values of J are small. The coefficients $C_0{}^+$ and $C_1{}^+$ have a shoulder at about 950 MeV/c. This effect, presumably related to the shoulder in the total cross section, does not appear in the higher coefficients, which suggests that it is caused by an interaction in a state having $J=\frac{1}{2}$.

C. Spin of $N^*(1688)$

In Fig. 14: (a) There are large peaks at 1030 MeV/c in $C_0{}^-$ to $C_5{}^-$, (b) $C_6{}^-$ and $C_7{}^-$ are small but not negligible, (c) $C_8{}^-$ and $C_9{}^-$ are not significantly different from zero.

The simplest explanation of these features is that there is a large $D_{5/2}$-$F_{5/2}$ interference term present, with a resonance in at least one of these states.[7] Comparison of the present data with results from charge-exchange scattering[2] indicates that both the $D_{5/2}$ and $F_{5/2}$ amplitudes are predominantly in the $T=\frac{1}{2}$ state. This is shown by writing the differential cross sections in terms of the scattering amplitudes a_1 and a_3 for states having isotopic spin $\frac{1}{2}$ and $\frac{3}{2}$, respectively,

$$d\sigma/d\Omega(\pi^-p\rightarrow\pi^-p)=\tfrac{1}{9}[|a_3|^2+4|a_1|^2+4\,Re(a_1{}^*a_3)],$$
$$d\sigma/d\Omega(\pi^-p\rightarrow\pi^0n)=\tfrac{1}{9}[2|a_3|^2+2|a_1|^2-4\,\mathrm{Re}(a_1{}^*a_3)].$$

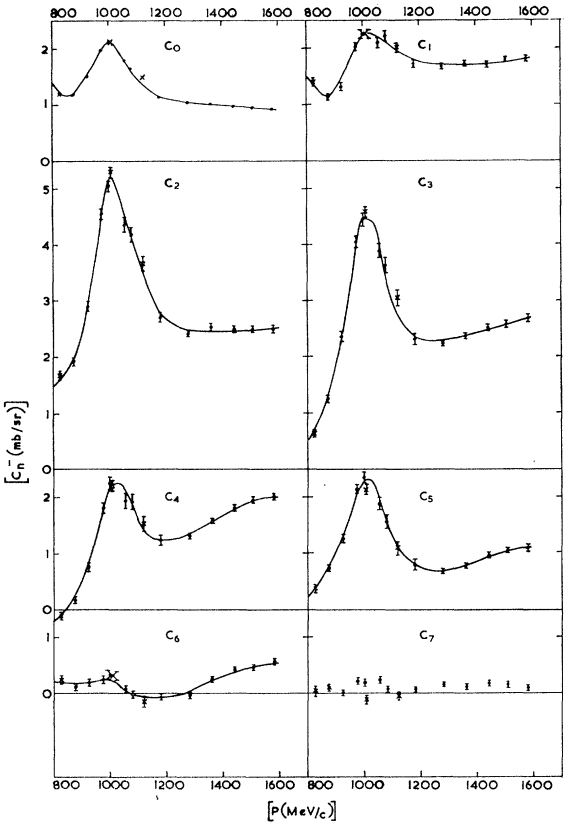

FIG. 14. Expansion coefficients for π^-p elastic scattering obtained from 7th-order fits at all momenta. The points denoted by crosses at 827, 1003, and 1121 MeV/c are taken from Helland *et al.* (Ref. 7).

The value of C_5^0 for charge exchange scattering has a peak of 0.60±0.15 mb. This is consistent with the peak above the background in C_5^- of about 1.5 mb observed in this experiment, if both amplitudes have $T=\frac{1}{2}$.

Finally it is interesting to note that the behavior of C_6^- is readily explained as a consequence of interference between the real part of a $J=\frac{5}{2}$, $I=\frac{1}{2}$ resonant amplitude for $N^*(1688)$ and the real part of a $J=\frac{7}{2}$, $I=\frac{3}{2}$ amplitude describing the $N^*(1928)$, provided that these have the same parity.

A more detailed discussion of the interpretation of the results of this experiment will be given in a paper (to be published) describing polarization measurements in the same momentum range.

VIII. CONCLUSIONS

$N^*(1688)$ has $I=\frac{1}{2}$, $J=\frac{5}{2}$; $N^*(1928)$ has $I=\frac{3}{2}$, $J=\frac{7}{2}$. The two resonances probably have the same parity.

ACKNOWLEDGMENTS

We are grateful for the friendly cooperation of the Nimrod operating crew and of the High-Energy Physics Engineering Group. Their assistance, particularly in the early days of operation of Nimrod, was a major contribution to the successful completion of the experiment. We are also grateful to P. J. Coleman, C. R. Cox, N. A. Cumming, R. Downton, K. S. Heard, R. Mackenzie, Miss J. Robertson, D. C. Salter, and D. C. Thomas for invaluable assistance in setting up the experiment and taking data.

PHYSICAL REVIEW VOLUME 149, NUMBER 4 30 SEPTEMBER 1966

Pion-Pion Interactions in $\pi^- p$ Reactions at 2.1 BeV/c*

E. WEST,† J. H. BOYD, A. R. ERWIN, AND W. D. WALKER
University of Wisconsin, Madison, Wisconsin
(Received 28 April 1966)

An analysis is given of the interactions of two pions as they result from the reactions of negative pions incident upon protons with a momentum of 2.1 BeV/c. A historical background of the motivation for the experiment is given and experimental techniques for dealing with the data are described, from the points of view of both event-by-event analysis and the physical theories which aid in the understanding of the results. Cross sections are given for the various reactions and are inferred by Chew-Low methods for pion-pion scattering. Evidence is presented which indicates that two resonant states in addition to the ρ meson and $N_{3/2}^*(1238)$ are present in these reactions: (1) the $N_{3/2}^*(1920)$, whose existence in other reactions is well established, and (2) the $T=0$, s-wave pion-pion interaction, which is still in doubt, known as the ϵ^0, the evidence for which stems from an analysis of the decay distribution of the ρ^0. Finally, corrections to the one-pion-exchange model which involve pion-nucleon scattering vertices are made in an attempt to determine more accurately the low-energy, $T=0$, s-wave pion-pion scattering cross sections, the results suggesting a range of about 10–15 mb in the region below the ρ.

I. INTRODUCTION

THE development of bubble chambers, and especially of liquid-hydrogen bubble chambers, has allowed the accumulation of a vast body of empirical data involving inelastic interactions between fundamental particles.

Many of the properties of these resonances are well measured and in several cases accurate predictions were made on the basis of earlier data. For example, the earliest data on pion production in pion-nucleon collisions indicated that above an energy of 1 BeV a small momentum transfer to the nucleon is preferred.[1] This observation has led directly to our present recognition that the one-pion-exchange (OPE) interaction is an important part of the over-all process. Physically this can be imagined as an incident pion striking a target furnished in a virtual state by the nucleon.

Analysis of electromagnetic data also implied that there must be a strong pion-pion interaction[2,3] which, in fact, probably had the form of a resonance in the $T=1$, $J=1$ and $T=0$, $J=1$ states.[3] In addition a π-P phase-shift analysis was used to deduce an energy for the resonance of about 660 MeV.[4] Other data indicated a peak in the spectrum at an energy near 600 MeV.[5]

* Work supported in part by the U. S. Atomic Energy Commission under contract No. AT(11-1)-881, COO-881-59.

† Now at the University of Toronto, Toronto, Ontario, Canada.

[1] L. M. Eisberg, W. B. Fowler, R. M. Lea, W. D. Shephard, R. P. Shutt, A. M. Thorndike, and W. L. Whittmore, Phys. Rev. **97**, 797 (1955); W. D. Walker and J. Crussard, *ibid.* **98**, 1416 (1955).

[2] W. Holladay, Phys. Rev. **101**, 1198 (1956).

[3] W. R. Frazer and J. R. Fulco, Phys. Rev. Letters **2**, 365 (1959).

[4] J. Bowcock, N. Cottingham, and D. Lurie, Phys. Rev. Letters **5**, 386 (1960); Nuovo Cimento **19**, 142 (1961). Also see J. A. Anderson, Vo X. Bang, P. G. Burke, D. D. Carmony, and N. Schmitz, Phys. Rev. Letters **6**, 365 (1961).

[5] E. Pickup, F. Ayer, and E. O. Salant, Phys. Rev. Letters **5**, 161 (1960); in *Proceedings of the Tenth Annual International Conference on High Energy Physics at Rochester* (Interscience Publishers, Inc., New York, 1960); see also F. Bonsignori and F. Selleri, Nuovo Cimento **15**, 465 (1960).